An Aqueous Channel for Filamentous Phage Export
Denise K. Marciano, *et al.*
Science **284**, 1516 (1999);
DOI: 10.1126/science.284.5419.1516

Europa, which might persist for decades after local geological activity has ceased (*31*). We have not detected any such endogenic hot spots. Upper limits to hot spot circular-equivalent diameter and temperature in the 18% of Europa's surface covered by our most sensitive observations (the low-latitude nighttime coverage shown in Fig. 1) are 16.8 km at 130 K, 6.2 km at 200 K, 3.4 km at 273 K, or 2.0 km at 350 K. This is much fainter than a brief thermal event tentatively identified in 1981 ground-based observations (*32*).

References and Notes

1. R. T. Pappalardo *et al.*, *J. Geophys. Res.*, in press; M. H. Carr *et al.*, *Nature* **391**, 363 (1998); R. Greeley *et al.*, *Icarus* **135**, 4 (1998).
2. W.-H. Ip *et al.*, *Geophys. Res. Lett.* **25**, 829 (1998).
3. J. R. Spencer, *Icarus* **69**, 297 (1987).
4. R. N. Clark, F. P. Fanale, A. P. Zent, *ibid.* **56**, 233 (1983).
5. J. R. Spencer, dissertation, University of Arizona, Tucson (1987).
6. In radiometric mode, PPR is a single-element bolometer with a circular field of view that is 2.5 mrad in diameter, which maps thermal emission from its targets by raster scanning of the Galileo scan platform on which it is mounted [E. E. Russell *et al.*, *Space Sci. Rev.* **60**, 531 (1992)]. Absolute calibration is provided by an on-board blackbody reference, prelaunch calibration, and observations of deep space and has errors that are currently $\leq$3 K. Problems with the filter wheel have limited the choice of filters on each orbit. The maps presented in Fig. 1 were produced by median-filtering the PPR observations to reduce radiation noise and then averaging all PPR observations whose fields of view overlap each point on the map.
7. G. S. Orton, J. R. Spencer, L. D. Travis, T. Z. Martin, L. K. Tamppari, *Science* **274**, 389 (1996).
8. S. G. Warren, *Appl. Opt.* **23**, 1206 (1984).
9. The brightness temperature of a body is the temperature of a blackbody with the same thermal emission brightness. For $\varepsilon = 0.9$, kinetic temperatures will be higher than broadband brightness temperatures by the factor $0.9^{-0.25}$, or 1.027.
10. The open filter is sensitive to Jupiter-shine reflected from Europa's nightside in addition to thermal radiation. Calculations based on daytime observations show that the Jupiter-shine contribution to apparent brightness temperatures will be $<$0.3 K before dawn and $<$1.0 K after sunset. Because albedo on scales of 100 km or larger varies by less than a factor of 2 on Europa, apparent local postsunset temperature variations due to local albedo variations will be $<$0.5 K. Tests using Voyager Europa spectra show that broadband and 27.5-μm brightness temperatures generally agree to $\leq$1 K.
11. D. Morrison, in *Planetary Satellites*, J. Burns, Ed. (Univ. of Arizona Press, Tucson, AZ, 1977), pp. 269–301. Thermal radiation varies considerably with longitude, peaking near longitude 270°.
12. D. L. Blaney, J. D. Goguen, G. J. Veeder, T. V. Johnson, D. L. Matson, *Lunar Planet. Sci.* **XXX** (CD-ROM, abstr. 1657)(1999).
13. A. E. Wechsler, P. E. Glaser, J. A. Fountain, in *Thermal Characteristics of the Moon*, J. W. Lucas, Ed. (MIT Press, Cambridge, MA, 1972), pp. 215–241.
14. R. H. Brown and D. Matson, *Icarus* **72**, 84 (1987).
15. M. L. Urquhart and B. M. Jakosky, *J. Geophys. Res.* **101**, 21169 (1996).
16. P. Helfenstein *et al.*, *Icarus* **135**, 41 (1998); D. L. Domingue, B. W. Hapke, G. W. Lockwood, D. T. Thomson, *ibid.* **90**, 30 (1991).
17. B. J. Buratti and J. Veverka, *ibid.* **55**, 93 (1983).
18. "Postsunset" observations cover a range of local time (measured in degrees of rotation after midnight) of 270° through 345°, from 0 to 18 hours after sunset. Similarly, "predawn" observations cover local times of 30° through 90°, from 14 to 0 hours before sunrise. At the equator, europan day and night each last 1.775 Earth days.
19. A. S. McEwen, *J. Geophys. Res.* **91**, 8077 (1986).
20. The Voyager images used by McEwen (*19*) at longitudes 0° through 75°W were taken at solar phase angles of 3° and 12° and do not show bolometric albedo, which accounts for light reflected in all directions. Variations in light-scattering properties at a high solar phase angle might produce variations in bolometric albedo that are not apparent in these images, but unrealistically large scattering variations would be required to reverse the trend of albedo with latitude, as would be required if albedo was the direct cause of the observed postsunset temperature variations.
21. J. M. Saari and R. W. Shorthill, *Icarus* **2**, 115 (1963); R. L. Wildey, B. C. Murray, J. A. Westphal, *J. Geophys. Res.* **72**, 3743 (1967).
22. The resolution (12 km per pixel) of the best Galileo images of this area is sufficient to distinguish major ridge systems and show the location of chaotic terrain, which is revealed by its low albedo and mottled appearance.
23. G. B. Hansen, personal communication.
24. J. Eluszkiewicz, *J. Geophys. Res.* **96**, 19217 (1991); R. B. Alley *et al.*, *J. Glaciol.* **32**, 415 (1986).
25. M. K. Pospieszalska and R. E. Johnson, *Icarus* **78**, 1 (1989).
26. M. G. Kivelson *et al.*, *Science* **276**, 1239 (1997).
27. G. W. Ojakangas and D. J. Stevenson, *Icarus* **81**, 220 (1989).
28. P. V. Hobbs, *Ice Physics* (Oxford Univ. Press, London, 1974).
29. K. K. Williams and R. Greeley, *Geophys. Res. Lett.* **25**, 4273 (1998); J. M. Moore *et al.*, *Icarus* **135**, 127 (1998).
30. S. W. Squyres *et al.*, *Nature* **301**, 225 (1983); M. N. Ross and G. Schubert, *ibid.* **325**, 133 (1987).
31. J. E. VanCleve, in preparation. For a surface heated only by sunlight, the maximum possible equatorial nighttime temperature (assuming zero albedo and infinite thermal inertia) is 130 K, and warmer nighttime temperatures would be an unambiguous sign of endogenic activity.
32. W. C. Tittemore and W. M. Sinton, *Icarus* **77**, 82 (1989). This event, if real and thermal in origin, implied a region with a diameter of 176 km at 273 K or a region of 52 km at 350 K.
33. C. Phillips, personal communication.

34. This work was supported by the Galileo project and NASA grant NAG5-6794. We thank L. Barnard and O. Liepack for assistance with design and implementation of the observation sequences and the entire Galileo team at the Jet Propulsion Laboratory for making the Galileo mission a success. The paper benefited from comments by R. Pappalardo, P. Geissler, and D. Domingue.

14 January 1999; accepted 14 April 1999

An Aqueous Channel for Filamentous Phage Export

Denise K. Marciano, Marjorie Russel,* Sanford M. Simon*

Filamentous phage f1 exits its *Escherichia coli* host without killing the bacterial cell. It has been proposed that f1 is secreted through the outer membrane via a phage-encoded channel protein, pIV. A functional pIV mutant was isolated that allowed *E. coli* to grow on large maltodextrins and rendered *E. coli* sensitive to large hydrophilic antibiotics that normally do not penetrate the outer membrane. In planar lipid bilayers, both mutant and wild-type pIV formed highly conductive channels with similar permeability characteristics but different gating properties: the probability of the wild-type channel being open was much less than that of the mutant channel. The high conductivity of pIV channels suggests a large-diameter pore, thus implicating pIV as the outer membrane phage-conducting channel.

The pIV protein is one of three filamentous phage proteins that are not part of the f1 virion but are required for phage export from the host bacterium. Interest in pIV has been stimulated by its sequence similarity to proteins in the type IV pilus assembly and in transport pathways, including type II and type III secretion systems (*1*). Both of these complex secretion systems mediate the export of proteins in Gram-negative bacteria. In type II secretion, toxins or degradative enzymes are secreted into the extracellular milieu; in type III secretion, proteins are secreted and injected directly into the cytosol of eukaryotic host cells, causing cytotoxicity. Bacteria with type II or type III secretion systems include such notorious animal and plant pathogens as *Yersinia*, *Salmonella*, *Shigella*, and *Erwinia*, all of which express a pIV homolog necessary for secretion or virulence. Although it has been postulated that pIV and its homologs function as outer membrane channels, there has been no direct evidence to support this hypothesis.

The pIV protein exists as a large homomultimer in the outer membrane of *E. coli*. Purified multimers are large cylindrical structures, as viewed by scanning transmission electron microscopy (STEM) (*2*). The filamentous phage is approximately 1 μm long with a diameter of 6 to 7 nm. A simple diffusion pore 6 to 7 nm in diameter would cause *E. coli* to be very sensitive to external stresses. However, phage-infected *E. coli* maintain long-term viability. Thus, if pIV were to form a channel, it would most likely be opened only during phage export by a gating mechanism.

The Rockefeller University, 1230 York Avenue, New York, NY 10021, USA.

*To whom correspondence should be addressed. E-mail: russelm@rockvax.rockefeller.edu (M.R) and simon@rockvax.rockefeller.edu (S.M.S.)

We used two assays to test whether pIV increased the permeability of the *E. coli* outer membrane: sensitivity to large antibiotics and growth on large carbohydrates. Vancomycin is an antibiotic that cannot cross the bacterial outer membrane because of its hydrophilicity and large size [molecular weight (MW) = 1449]. Wild-type pIV (pIV^+) and pIV with a point mutation at $Ser^{324} \rightarrow Gly^{324}$ (pIV^{S324G}), which still functioned for phage export, were synthesized from plasmids at slightly lower levels than in phage-infected cells (*3*). Expression of pIV^{S324G} substantially increased the sensitivity of *E. coli* to vancomycin, whereas pIV^+ did not (Fig. 1A) (*4*). Even without vancomycin, bacteria with pIV^{S324G} did not grow well. However, their growth defect was fully rescued by the addition of 20% sucrose, an osmoprotectant that does not cross the inner membrane, further suggesting that pIV^{S324G} makes the outer membrane permeable (*3*). The pIV^{S324G} made bacteria sensitive to concentrations of vancomycin 100-fold lower than those affecting *envA* and *tolQ* mutants, which are known to have leaky outer membranes (*5*). Experiments with bacitracin (MW = 1411) gave similar results as the vancomycin experiments (*3*).

To test if pIV increased the permeability to carbohydrates, we expressed pIV in the strain MCR106, which has a 501–base pair internal deletion of the gene *lamB* encoding an outer membrane maltoporin (*6*), and grew the strain on plates containing sugars of increasing size (Fig. 1B). In the absence of LamB, *E. coli* are unable to grow on maltodextrins larger than maltotriose (*7*). *Escherichia coli* expressing low levels of pIV^{S324G} grew on 0.2% sugars up to maltohexaose (*8*). They also grew on maltoheptaose, albeit poorly, when sugar concentrations were increased to 0.4% (*3*). Bacteria expressing pIV^+ grew poorly on maltotriose and did not

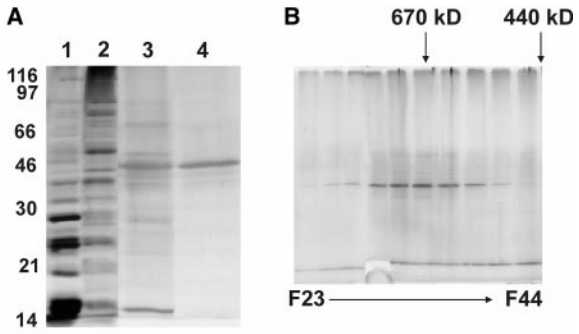

Fig. 2. Purification of mutant pIV. (**A**) Silver-stained SDS–polyacrylamide gel electrophoresis (SDS-PAGE) gel showing major purification steps. His-tagged pIV^{S324G} was expressed from plasmid $pPMR132^{S324G}$ in strain K1312 (MC4100 *ompR::Tn10*). Lane 1 (1× load), total cell lysate; lane 2 (4×), solubilized membranes; lane 3 (40×), elution from the Ni^{2+}-Sepharose column; and lane 4 (40×), pooled peak fractions from the BioGelA5M column. (**B**) Silver-stained SDS-PAGE gel showing the elution profile of pIV from the BioGel column. Gel filtration standards are indicated. Purification of wild-type pIV was similar (*3*). F23 through F44 indicate the fractions analyzed.

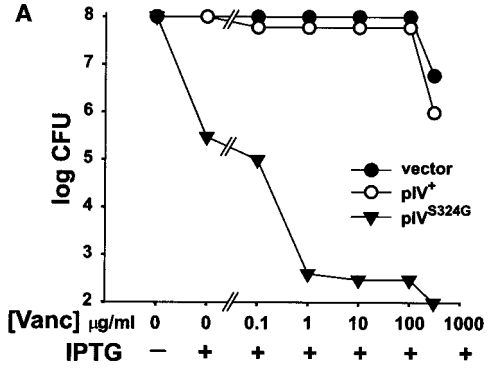

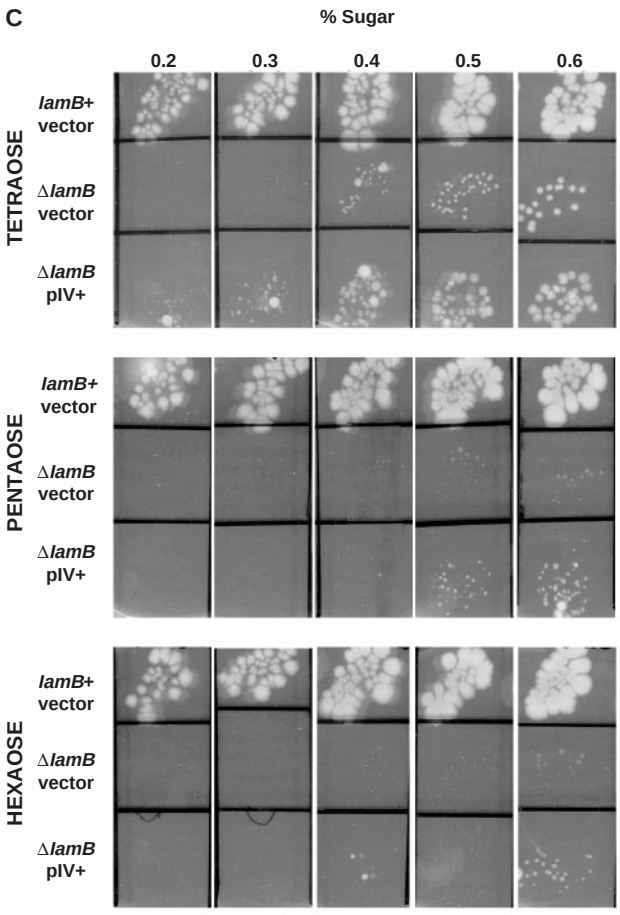

Fig. 1. Vancomycin sensitivity and growth on maltodextrins. (**A**) Serial dilutions of *E. coli* strain K1712 containing the indicated plasmid were plated on tryptone broth plates ± 1 mM IPTG and increasing concentrations of vancomycin. Colony-forming units (CFU) were determined after 24 hours at 37°C. (**B**) Cultures of MC4100 pPMR131 ($lamB^+$, empty vector), MCR106 pPMR131 (Δ*lamB*106, empty vector), MCR106 pPMR132 (Δ*lamB*106, pIV^+), and MCR106 $pPMR132^{S324G}$ (Δ*lamB*106, pIV^{S324G}) were washed with M63 salts, and plated on minimal media containing M63 salts, 10 μM IPTG, 50 μg/ml chloramphenicol, and 0.2% (w/v) of the indicated sugar. Growth was assessed after 36 hours at 37°C. Shown is one of three similar experiments. (**C**) The same strains as in (B) (minus MC4100Δ*lamB*106, pIV^{S324G}) were washed and plated on minimal media containing M63 salts, 1 mM IPTG, 50 μg/ml chloramphenicol, and the indicated sugar. Growth was assessed after 6 days at 37°C. Shown is one of three similar experiments.

grow on the larger maltose sugars under these conditions.

Escherichia coli expressing pIV$^+$ grew on maltodextrins larger than maltotriose only when both the sugar concentration and growth time were increased (Fig. 1C). Under these conditions, pIV$^+$ conferred a growth advantage over the empty vector control. As the sugar size increased, bacteria with pIV$^+$ required higher sugar concentrations to grow; colonies could be seen on maltohexaose only when the concentration was increased to 0.6%. The modest growth advantage due to pIV$^+$ was not the result of mutation, because all of the plated cells formed colonies and these bacteria grew just as slowly after restreaking (*9*).

To directly test for channel activity in electrophysiological assays, we purified His-tagged pIV$^+$ and pIV^{S324G} and reconstituted them into proteoliposomes (*10*). The pIV proteins were purified by nickel-chelate and size exclusion chromatography (Fig. 2). Both wild-type and mutant proteins eluted in similar fractions corresponding to ~670 kD, indicating that they exist as multimers of similar size. In addition, both forms of pIV appeared similar by negative staining electron microscopy (*3*). Both His-tagged proteins were functional, as assessed by their ability to function in phage export (*11*). Proteoliposomes with pIV^{S324G} were fused to planar lipid bilayers. Large, single channels were observed at positive and negative voltages ($+V_m$ and $-V_m$) (Fig. 3, A and B). Initially, an additional smaller channel was observed that had characteristics similar to those previously reported for OmpC (*12*). Subsequently, pIV was purified from an *E. coli ompR* strain, which contains low amounts of the porins OmpC and OmpF. The ratio of porin to pIV from cell lysates of the *ompR* strain was 50 times lower than in the original strain (*3*), and contaminating channels were very rarely observed after purification. A recording of pIV^{S324G} channels with a contaminating channel illustrates the markedly greater current through pIV channels (Fig. 3A). Both pIV^{S324G} and pIV$^+$ independently displayed

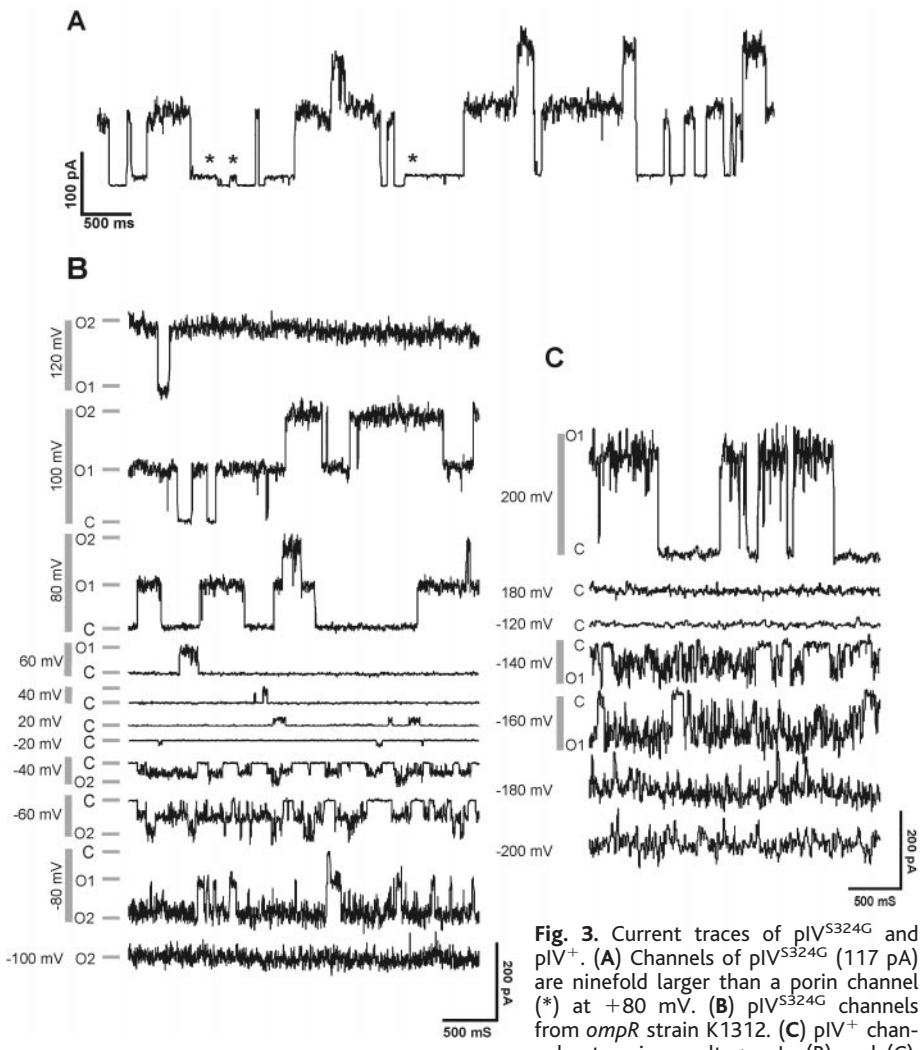

Fig. 3. Current traces of pIV^{S324G} and pIV$^+$. (**A**) Channels of pIV^{S324G} (117 pA) are ninefold larger than a porin channel (*) at +80 mV. (**B**) pIV^{S324G} channels from *ompR* strain K1312. (**C**) pIV$^+$ channels at various voltages. In (B) and (C), the traces were vertically displaced for clarity and marked as closed (C), or with one (O1) or two (O2) open channels. The solution for (A) was 285 mM NaCl in the *cis* and 150 mM in the *trans* chamber. In (B) and (C), 150 mM KCl was in both chambers. All solutions contained 10 mM NaHepes (pH 7.4), 5 mM $MgCl_2$, and 5 mM $CaCl_2$.

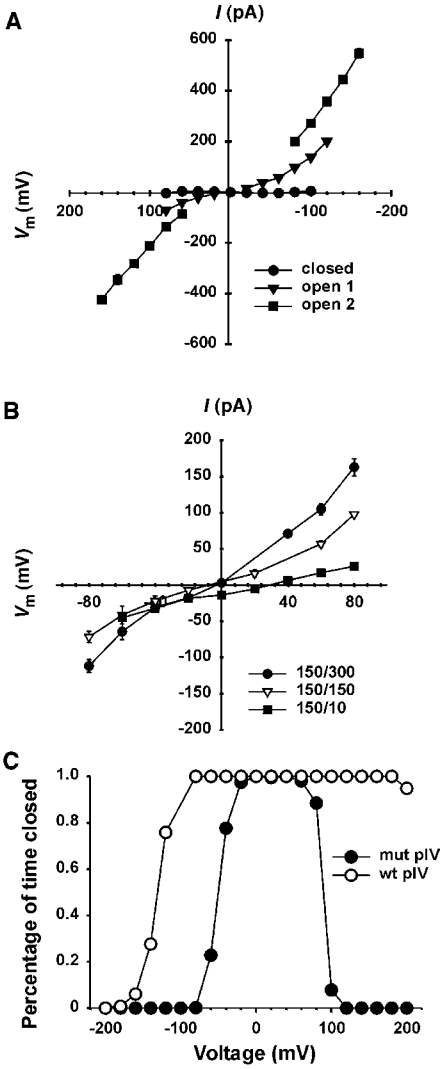

Fig. 4. Current-voltage relationships of pIV^{S324G}. (**A**) The average current for the closed, single open (O1), and double open (O2) pIV^{S324G} channels in 150 mM salt (*cis* and *trans*) was plotted. (**B**) The O1 currents for pIV^{S324G} channels were measured in salt gradients of 150/10, 150/150, and 150/300 mM KCl in the *cis* and *trans* chambers, respectively. Both chambers had 10 mM KHepes (pH 7.4), 5 mM $MgCl_2$, and 5 mM $CaCl_2$. In (A) and (B), each data point is the current average ± SD calculated from an all-points histogram from several traces of a single experiment. Shown is one of five similar experiments. (**C**) Probability of time in the closed state (P_{closed}) for mutant and wild-type pIV. The voltage was increased in 20-mV steps with a return to 0 mV between each step. We calculated P_{closed} from an all-points amplitude histogram of a 2-min recording for each voltage: $P_{closed} = \Sigma t_{closed} / \Sigma t_{closed} + t_{open}$. Experiments were done in 150 mM KCl, 10 mM NaHepes (pH 7.4), 5 mM $MgCl_2$, and 5 mM $CaCl_2$. Shown is one of two similar experiments.

the same channel behavior when purified from either strain (*3*).

Most attempts to detect channels with pIV^{S324G} were successful ($n > 40$). At low voltages (-20 mV $< V_m <$ $+40$ mV) there were occasional channel openings (Figs. 3B and 4C). At intermediate voltages ($V_m < -20$ mV or $V_m > +50$ mV) channels opened to two different current levels, O1 and O2, where O2 was double the size of O1. At larger voltages ($V_m < -80$ mV or $> +120$ mV) only the larger O2 current level was observed. When several pIV multimers were incorporated into the bilayer, the maximum current was a multiple of the O2 current. This suggests that a pIV multimer has two conductance states or that the multimers reconstitute in pairs.

There were three distinct effects of voltage on the activity of the channel. First, at positive potentials, the channels required a greater voltage to open than at negative potentials. Second, the single-channel conductance of pIV^{S324G} was larger at $+V_m$ than it was at $-V_m$. This can be seen both in the single-channel recordings (Fig. 3B) and in the current-voltage plot, where opening to the first conductance level (O1) was 1.22 ± 0.03 nS ($\pm$SD) at 80 mV and 0.90 ± 0.10 nS at -80 mV in 150 mM KCl (Fig. 4A). The asymmetric response to the polarity of the voltage suggests that pIV^{S324G} channels reconstitute into the lipid bilayer with a common asymmetry. Third, the channel conductance increased with increasing voltage. The selectivity of pIV^{S324G} channels was determined by two criteria: quantification of channel current and reversal potential in varying salt solutions (Fig. 4B). They were approximately four times more permeable to potassium than to chloride.

In contrast to pIV^{S324G}, channels from pIV^+ ($n = 7$) were observed only at very high voltages ($V_m > 180$ mV or $V_m < -120$ mV), which made them more difficult to characterize. For a given voltage, the O1 conductance for pIV^+ was less than that for pIV^{S324G}. At $+200$ mV, the O1 conductance of pIV^+ was 1.2 ± 0.2 nS (*13*) and the percentage of time open was 5% (Fig. 4C). At $+80$ mV, the pIV^{S324G} channel conductance and probability of being open closely resembled that of pIV^+ at $+200$ mV. Thus, the pIV^{S324G} channel behaved as if the mutation shifted its voltage dependence, thereby increasing the likelihood of the channel being open at lower voltages.

The channels formed by pIV^{S324G} and pIV^+ have many features in common. (i) Both reconstitute into membranes with a common asymmetry, with a larger channel conductance at $+V_m$ than $-V_m$. (ii) Both have similar cationic selectivity. (iii) Both have a greater probability of opening when at greater V_m. (iv) Both are more likely to open when V_m is negative (Fig. 4C). (v) Both channel conductances increase with increasing V_m. (vi) Both are extremely large channels in comparison to known porin molecules such as OmpC, whose conductance is 110 pS at 150 mM KCl (*12*). The primary difference between pIV^{S324G} and pIV^+ channels is their probability of opening. This difference confirms that the channel activity is due to pIV and not a contaminant.

The pIV pore diameter is estimated to be 6 nm if it is assumed that a pIV multimer has two conductance states (*14*). This diameter is large enough to accommodate an extruding phage (6 to 7 nm) and is consistent with measurements of pIV pore diameter (7 to 8 nm) in the STEM (*2*). The pIV^{S324G} is open much more frequently than pIV^+ at voltages likely to exist across the outer membrane (*15*). This is consistent with the growth and antibiotic sensitivity experiments, indicating that the electrophysiological recordings reflect the in situ behavior of the protein. It is also consistent with pIV^+ being a tightly gated channel. Transmembrane aqueous channels have been shown to function in the transport of ions and metabolites and the translocation of DNA and unfolded proteins (*16, 17*). The sequence similarity between pIV and numerous proteins involved in pilus assembly or secretion of folded proteins (*18*) suggests that use of large, gated channels may be a general mechanism for supramolecular transport.

References and Notes

1. M. Russel, *J. Mol. Biol.* **279**, 485 (1998); C. J. Hueck, *Microbiol. Mol. Biol. Rev.* **62**, 379 (1998).
2. N. A. Linderoth, M. N. Simon, M. Russel, *Science* **278**, 1635 (1997).
3. D. K. Marciano, M. Russel, S. M. Simon, unpublished observations.
4. *Escherichia coli* containing a mutagenized population of gene IV were originally screened for sensitivity to the detergent deoxycholate [M. Russel, N. A. Linderoth, A. Sali, *Gene* **192**, 23 (1997)]. pIV^{S324G} was chosen because it was sensitive to deoxycholate, yet still functioned in phage export. For the vancomycin assay, we used strain K1712 [*HfrC* (λ) *tonA22 garB10 ompF relA1 pit10 spoT1* $T2^r$ *fadL701 phoM510 mcrB rrnB2 slyD::kan rcsA::tet*] with gene IV expressed from plasmid pPMR129 under the control of the isopropyl-β-D-thiogalactopyranoside (IPTG)–inducible *tac* promoter.
5. R. E. Webster, *Mol. Microbiol.* **5**, 1005 (1991); K. Young and L. L. Silver, *J. Bacteriol.* **173**, 3609 (1991).
6. MCR106 is MC4100 (F^- *ara*Δ139 *lac*U169 *rel*A *thi rps*L) Δ*lamB*106 [S. D. Emr and T. J. Silhavy, *J. Cell Biol.* **95**, 689 (1982)].
7. C. Wandersman, M. Schwartz, T. Ferenci, *J. Bacteriol.* **140**, 1 (1979).
8. Colonies with pIV^{S324G} had a mucoid phenotype, making it impossible to relate colony size to bacterial number (Fig. 1B). The cell number per colony decreased with increasing sugar size for all strains.
9. Large colonies from the pIV^+ culture appeared on plates with tetraose and larger sugars at low frequency. Thus, the maltodextrin growth assay may be useful for selection of pIV mutants with increased permeability as well as for determining in vivo outer membrane permeability.
10. Purification was a modification of (*2*). Briefly, cells were lysed by French press and membranes were isolated by centrifugation onto a 60% (w/v) sucrose cushion. Membranes were solubilized [4% octyl-polyoxyethylene (w/v), 50 mM tris-Cl (pH 8.0), 500 mM NaCl, 30 mM imidazole, 2 mM benzamidine] and bound to Ni^{2+}-Sepharose beads. The pIV was eluted in buffer [1% CHAPS (w/v), 400 mM imidazole, 50 mM tris-Cl (pH 8.0), 500 mM NaCl, 2 mM benzamidine]. The fractions containing pIV were pooled, concentrated, and chromatographed on a BioGelA5M column [1% CHAPS (w/v), 25 mM NaHepes (pH 8.0), 500 mM NaCl, 0.5 mM NaEDTA (pH 8.0), 2 mM benzamidine]. Liposomes containing 12 mM lipid (egg phosphatidylcholine and egg phosphatidic acid in a 9:1 ratio) were bath sonicated for 5 min, freeze-thawed 10 times, and repeatedly extruded through membranes with 200-nm pores (Lipsofast; Avestin Inc.). We added β-octyl glucoside to a concentration of 22.5 mM. Purified pIV was added to liposomes at ~1:200 (v/v) to give a final pIV concentration of 10 μg/ml in 12 mM lipids. Detergent was removed with Biobeads SM2 (Pharmacia). Planar lipid bilayers were formed by applying a 20 mg/ml lipid solution to a Teflon hole (100 to 250 μm in diameter) separating the *cis* and *trans* chambers as described (*17*). Lipids used were *E. coli* phosphatidylethanolamine, 1,2-diphytanoyl-*sn*-glycero-3-phosphocholine (DPPC), and brain phosphatidylserine (PS) in a 5:4:1 ratio; DPPC:PS in a 9:1 ratio; or total *E. coli* lipids (Avanti Polar Lipids). A bilayer 250 μm in diameter had a typical capacitance of 500 pF and conductance of <5 pS. Proteoliposomes were added to the *cis* chamber in the presence of a salt gradient. Solutions were stirred until fusion occurred, and then the gradient was dissipated. Data was acquired using an Axopatch 200 (Axon Instruments) and a 16-bit analog data acquisition board (National Instruments). Traces were filtered at 100 Hz. All data acquisition was controlled with software, developed by Yu Chen, written in LabView (National Instruments).
11. Dilutions of R484 phage (deleted for gene IV) were spotted on lawns of an F^+ derivative of MCR106 with plasmids $pPMR132^+$ or $pPMR132^{S324G}$ and IPTG. Bacteria can be infected with R484, but they cannot release progeny phage or form plaques unless complemented with functional pIV. Either His-tagged pIV^+ or His-tagged pIV^{S324G} was able to complement the defective phage and allow plaque formation.
12. A. H. Delcour, J. Adler, C. Kung, *J. Membr. Biol.* **119**, 267 (1991).
13. The conductance for pIV^{S324G} in the O1 state at $+200$ mV could be extrapolated to 1.7 nS from current-voltage plots. Because pIV^{S324G} is fully open in this range, actual channel transitions from the closed to the open state could not be measured.
14. If a channel is a cylindrical pore, its diameter can be estimated by [B. Hille, *Ionic Channels of Excitable Membranes* (Sinauer, Sunderland, MA, ed. 2, 1992)]
$$dpore = 2 \times [(\pi/2) + \sqrt{(\pi^2/4) + (4RL\pi/\rho)}]/(2R\pi/\rho)$$
Resistivity of the solution is $\rho = 77$ ohm·cm, pore length is $L = 7$ nm (measurements from STEM), and pore resistance is $R = 1/g$ where g is conductance. If the pIV multimer is a single channel with two conductance states (O1, O2), then $g = 3.4$ nS (160 mV, 150 mM KCl) and the estimated diameter is 6 nm. If a single current step (O1) corresponds to a single pIV multimer, then $g = 1.7$ nS and the estimated diameter is 4 nm. These values are only approximations.
15. J. B. Stock, B. Rauch, S. Roseman, *J. Biol. Chem.* **252**, 7850 (1977).
16. P. Boulanger and L. Letellier, *ibid.* **263**, 9767 (1988); H. Nikaido, *Mol. Microbiol.* **6**, 435 (1992); D. G. Thanassi *et al.*, *Proc. Natl. Acad. Sci. U.S.A.* **95**, 3146 (1998).
17. S. M. Simon and G. Blobel, *Cell* **65**, 371 (1991); *ibid.* **69**, 677 (1992).
18. T. R. Hirst and J. Holmgren, *Proc. Natl. Acad. Sci. U.S.A.* **84**, 7418 (1987); M. Sandkvist, M. Bagdasarian, S. P. Howard, V. J. DiRita, *EMBO J.* **14**, 1664 (1995).

19. We thank P. Model for continuous advice and helpful discussions. We also thank M. Shiloh and Y. Chen for helpful discussions and support; N. Linderoth, L. Boone, and J. Schmoranzer for preliminary experiments; S. Asheer for technical assistance; O. Anderson, M. Goulian, and R. MacKinnon for critical reading of the manuscript; T. Silhavy and S. Benson for strains; and L. Letellier and E. Kanner for suggestions. Supported by NIH Medical Science Training Program grant GM07739 (D.K.M.), NSF grant MCB93-16625 (M.R.), and the Keck Foundation (S.M.S.).

16 February 1999; accepted 26 March 1999